THE JOURNAL OF PHYSICAL CHEMISTRY B

Article

pubs.acs.org/JPCB

Molecular Mechanism of Direct Proflavine–DNA Intercalation: Evidence for Drug-Induced Minimum Base-Stacking Penalty Pathway

Wilbee D. Sasikala and Arnab Mukherjee*

Chemistry Department, Indian Institute of Science Education and Research, Pune-411021, India

Supporting Information

ABSTRACT: DNA intercalation, a biophysical process of enormous clinical significance, has surprisingly eluded molecular understanding for several decades. With appropriate configurational restraint (to prevent dissociation) in all-atom metadynamics simulations, we capture the free energy surface of direct intercalation from minor groove-bound state for the first time using an anticancer agent proflavine. Mechanism along the minimum free energy path reveals that intercalation happens through a minimum base stacking penalty pathway where nonstacking parameters (Twist→Slide/Shift) change first, followed by base stacking parameters (Buckle/Roll→Rise). This mechanism defies the natural fluctuation hypothesis and provides molecular evidence for the drug-induced cavity formation hypothesis. The thermodynamic origin of the barrier is found to be a combination of entropy and desolvation energy.

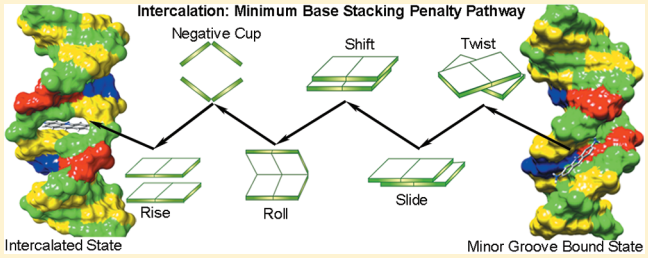

INTRODUCTION

DNA intercalation[1,2] (insertion between base pairs) is the mechanism by which a certain class of anticancer drugs functions.[3] Intercalation subsequently leads to inhibition of topoisomerase action followed by cell death.[4] It is also the preferred mode of binding of several proteins that control and regulate transcription.[5] Despite clinical and biophysical significance, the molecular mechanism of intercalation has eluded attention for several decades. Here, using extensive all-atom simulations, we capture for the first time direct intercalation of an intercalating drug proflavine in atomistic detail, depicting the molecular events encompassing the process. This study also addresses a long-standing debate on the intercalation mechanism and provides insight to make use in designing better and more efficient intercalators.

Fluorescence properties of the intercalating drugs enabled exhaustive thermodynamic and kinetic studies,[6−8] while structural investigations were carried out using NMR,[9] crystallographic studies,[10] molecular modeling,[11−13] force spectroscopic methods,[14] and so forth. Most of the kinetic studies on intercalation indicate that the process comprises *at least* two steps: a fast bimolecular outside binding, followed by a slow intercalation. The latter has two limiting hypotheses:[6] one in which DNA base pairs open up momentarily close to the bound drug allowing it to enter, and the other in which the drug forces the cavity in the DNA without requiring prior base pair opening. In this study, we provide direct molecular evidence for the second hypothesis, i.e., drug-induced cavity formation.

Intercalated state is the unique bound state (similar to the native state of a protein) compared to several possible unbound states (unfolded protein). The typical time scale for intercalation for small molecules is milliseconds.[6] Therefore, the direct intercalation process is extremely challenging to capture in computational studies. The first study on the molecular mechanism of intercalation by one of us was performed by deintercalation[15] (separating out the drug from the intercalation cavity), where we showed that daunomycin intercalation proceeds by binding to the minor groove of the DNA followed by an activated intercalation.[15] The emergence of a third step has been shown recently through conformational sampling of daunomycin and DNA.[16] While both the studies provide significant understanding toward the molecular detail of the process, a successful intercalation event that would suggest preintercalative mechanistic details, however, has not been achieved. Recent force-spectroscopic study indicated that intercalation and deintercalation are distinct processes and can occur in different time scales.[14]

Here we constructed for the first time a free energy surface (FES) of direct intercalation from the minor groove-bound state (MNS) for an anticancer[17] and antiviral[18] agent proflavine, using extensive all-atom simulations with well-tempered metadynamics[19] method. Metadynamics is an accelerated sampling method useful to explore the complex FES. It has been successfully applied to study several chemical and biological systems.[20] Well-tempered metadynamics[19] is an improvement over standard metadynamics because it provides control over the critical region (transition state) of the FES providing a physically viable mechanistic pathway (see Supporting Information (SI)).

Received: August 9, 2012
Published: September 14, 2012

COMPUTATIONAL DETAILS

Preparation of the MNS. A 12 base pair DNA, $d(GCGCTCGAGCGC)_2$, was created using the nucleic acid builder (NAB)[21] program. The AMBER99/parmbsc0 forcefield[22,23] has been used for the DNA. Since proflavine exists as a cation in the physiological system, the protonated form of proflavine was optimized followed by Merz-Kolmann charge calculation[24] using Hatree-Fock theory with 6-31G* basis set using Gaussian 03.[25] Antechamber module of AMBERTools[26] was used for restrained electrostatic potential charge (RESP)[27] calculation and generation of general amber force field (GAFF).[28] Finally, the coordinates and topology were converted to GROMACS format using amb2gmx.pl program.[29]

The MNS was created by docking using AutoDock software.[30,31] The AMBER charges of the nucleic acid atoms and quantum chemically derived charges for proflavine were kept unchanged during docking process. During the docking, proflavine was kept flexible, and DNA was kept rigid. The grid was generated on whole BDNA with grid points of 96, 104, and 96 in orthogonal directions, respectively, with a spacing of 0.54 Å, and the search was performed using the Genetic algorithm.[30] All 10 structures obtained after docking were MNSs, among which the best docked structure with a binding score of −6.25 kcal/mol was selected as the initial configuration of the MNS (X = 2.0 Å and φ = 76.9°).

Molecular Dynamic Simulation Protocol. The drug−DNA system was solvated by 11763 TIP3P water molecules[32] in a large cubic box of length 71.23 Å. Twenty-two sodium ions and one chloride ion were added to neutralize the system. The final system of 36096 atoms was energy minimized using the steepest descent method[33] followed by heating up to 300 K using a Berendsen thermostat[34] with a coupling constant of 0.2 ps and a harmonic restraint of 25 kcal/mol/Å^2 on heavy atoms of DNA and proflavine. After the energy minimization, the restraints were slowly reduced to 0.5 kcal/mol/Å^2 during a series of six simulations of 50 ps each at constant temperature 300 K and pressure 1 bar using a Berendsen thermostat and barostat,[34] followed by energy minimization for 1000 steps. Then a final unrestrained equilibration for 1 ns was done at constant temperature 300 K and 1 bar pressure using a Nose−Hoover thermostat[35,36] with a coupling constant of 0.2 ps and a Parrinello−Rahman barostat[37] with a coupling constant of 0.2 ps. The time step of each simulation was kept at 2 fs. Electrostatic interaction was treated using particle mesh Ewald (PME)[38] with a cutoff at 10 Å, and the van der Waals (vdW) cutoff was taken to be 10 Å.

Well-tempered metadynamics[19] was performed thereafter. It is a smoothly converging and tunable free energy method, which offers the possibility of controlling the regions of FES that are physically meaningful to explore and provides a unified framework of standard metadynamics and unbiased standard sampling.[19] We used a bias factor of 15 and added a Gaussian height of 0.048 kcal/mol at 2 ps intervals for intercalation and dissociation processes. Widths (σ) of the Gaussians were varied for different collective variables depending on the natural fluctuation observed in different states. For intercalation and dissociation, we used σ = 0.5 Å for X and σ = 0.2 radians for φ. The GROMACS[39] molecular dynamics program package was used to carry out the simulations. A separate program patch, PLUMED,[40] was used with modification to incorporate our collective variables to perform well-tempered metadynamics simulations.

Configurational Restraint. For simulations, a quartic potential[40] of the following form was used to apply configurational restraint:

$$V_{\text{wall}}(S) = \kappa(s - s_0)^4 \quad (1)$$

where κ represents the force constant taken to be 6 kcal mol^{-1} Å^{-2} in this study. s is a collective variable, and s_0 is the cutoff value where the potential has been applied.

MFEP Calculation and Cluster Analysis. We calculated the minimum free energy path (MFEP) for each process using the algorithm of Ensing et al.[41] Subsequently, we collected the structures that fall within a small deviation (dX, dφ) round each point, spaced to avoid overlap, along the MFEP. Then we performed cluster analysis of the structures collected around each point using a root-mean square deviation (rmsd) cutoff 1.0 Å. All the subsequent calculations of average properties and standard deviations of DNA parameters and energy components (plotted in Figure 3 and Figures S2 and S3) were performed using the members of the biggest cluster.

RESULTS AND DISCUSSION

We started well-tempered metadynamics simulation from the MNS in two coordinates X and φ (Figure 1a). X denotes the distance of proflavine from the DNA approximately perpendicular to the helical axis. φ measures the displacement of drug along the helical axis of the DNA. Therefore, φ can distinguish between intercalated ($\varphi \sim 0°$) and MNS ($\varphi \sim 90°$).

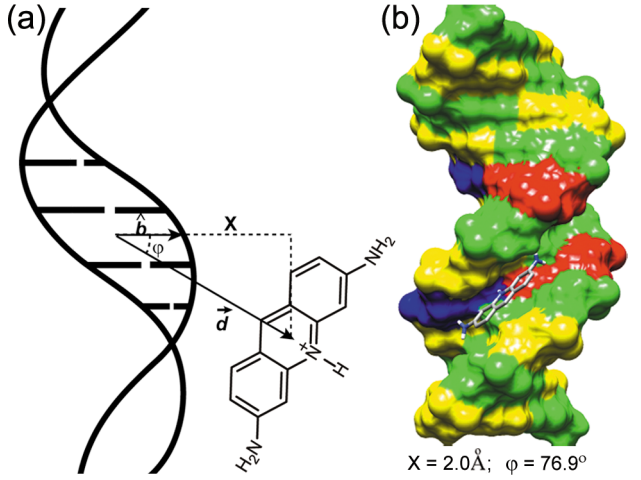

Figure 1. Schematic picture of the collective variables and initial drug−DNA configuration. (a) $\hat{b}$ is the unit vector from the COM of the IBPs consisting of four bases (C6,G7,C18,G19) to the COM of G7 and G19 ribose sugars that lie more toward the minor groove. $\vec{d}$ is the vector from the COM of IBP to the COM of proflavine. $X = \hat{b}\cdot\vec{d}$, $\varphi = \cos^{-1}(\hat{b}\cdot\vec{d}/|\vec{d}|)$. (b) Initial configuration of the docked MNS. Note the values of X and φ.

Expectedly, metadynamics simulation starting with the docked MNS along X and φ resulted in dissociation of the drug to a separated state. Figure 2a shows the FES for dissociation from the MNS. Configurational restraints were used (at $\varphi \geq 80°$ for MNS) to prevent the drug from going to the ends of DNA. Free energy of the MNS (ΔG_{MNS}) was −8.8 kcal/mol, in reasonable agreement with the experimental estimate of −6.8 kcal/mol[7].

To achieve intercalation, we now placed another configurational restraint along the distance between the intercalating

dx.doi.org/10.1021/jp307911r | J. Phys. Chem. B 2012, 116, 12208−12212

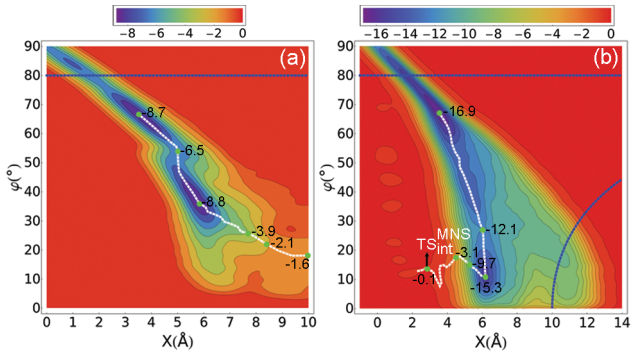

Figure 2. FES of (a) dissociation and (b) intercalation along X and φ. Free energy values are indicated by the labeled (kcal/mol) color bar on the top of each figure. White lines indicate the calculated MFEP. The green dots denote some representative points along each MFEP, the corresponding structures of which (for Figure 2b) are shown in Figure 4. The transition state for the intercalation process is labeled. Blue lines indicate the configurational restraint.

base pairs (IBPs) of DNA and the center of mass (COM) of the drug at 10 Å, apart from usual restraint on φ, to prevent dissociation of the drug (i.e., reducing configurational freedom at uninteresting part of the FES). The restraints were placed far away from the DNA so that the FES for intercalation was not affected. FES for the intercalation process through the minor groove is shown in Figure 2b. The intercalation barrier from the minor groove was thus found to be ($\Delta G^{\#,int}_{MNS}$) 16.9 kcal/mol (verified by additional FES construction from the unrelated initial condition shown in Figure S4), in good agreement with experiments (12.5−15.1 kcal/mol).[7,42,43] Simulation for intercalation process was stopped once the drug crossed the transition state after allowing sufficient time to recross. Continuing the simulation would populate the intercalated state until the drug deintercalates again. This deintercalation process was not studied here, as seen from Figure 2b where the stable intercalated state is not present.

In a multidimensional FES of a process, MFEP provides the statistically most favorable mechanistic picture. Therefore, we calculated the MFEP for intercalation from MNS using the algorithm by Ensing et al.,[41] previously applied to understand the dissociation mechanism of minor groove-bound drugs.[44] Structures were collected around discrete points along the MFEP (white lines in Figure 2), and, subsequently, cluster analyses[45] were performed. The average structural and energy components were calculated from the members of the biggest cluster (Figure 3) and plotted against the MFEP index (steps along the MFEP) taken to be 0 at the transition state and increasing toward the MNS. Energy parameters were calculated for a subsystem consisting of IBPs, drug, and the largest number of water in the first hydration shell (taken to be within 3.4 Å from the heavy atoms) at any point along the MFEP (to conserve mass for the subsystem). Here we assume that the part of the system uninvolved in the intercalation will not contribute in relative energy change.

Going along the MFEP of intercalation from the MNS, Figure 3a shows the various DNA base pair step parameters, and Figure 3b shows various average energy parameters for the

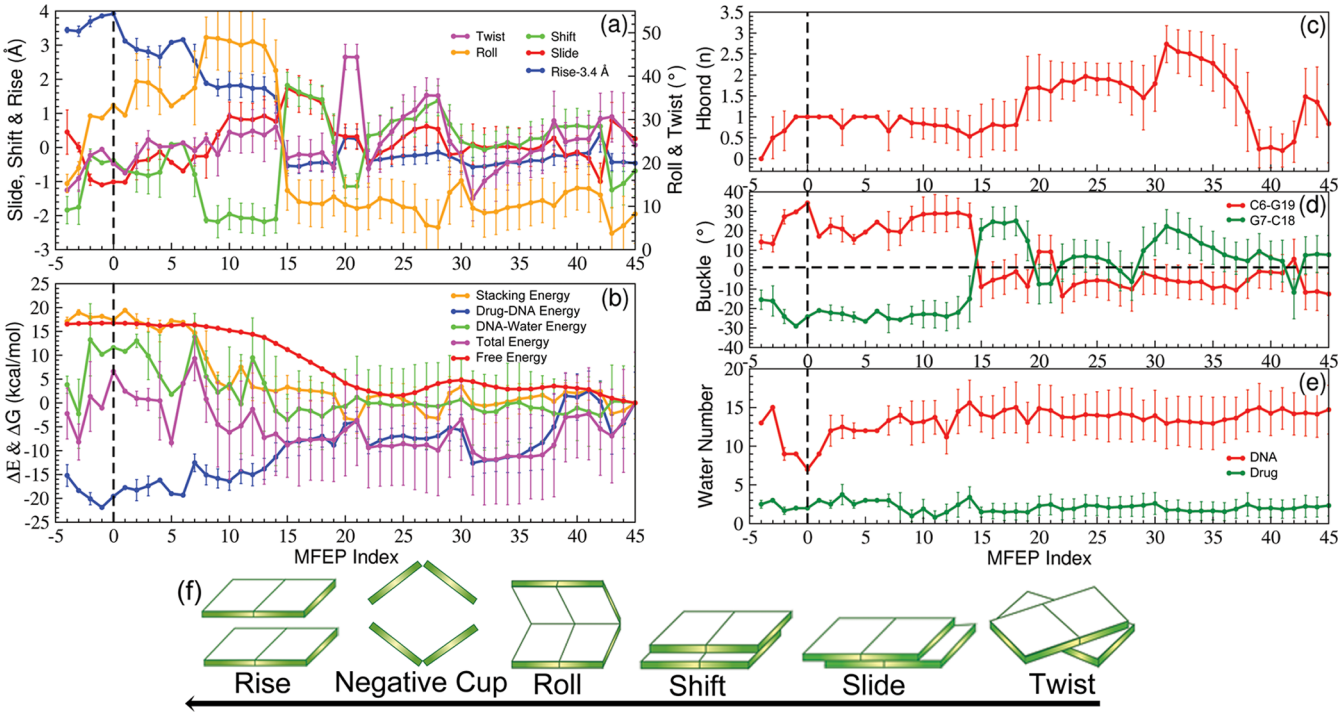

Figure 3. Analysis for the intercalation process from the MNS. (a) DNA base pair step parameters for the C6G7 base pair calculated using Curves +.[52] The vertical black dashed line represents the transition state. (b) Relative energy parameters (sum of vdW and Coulombic) taken to be zero at the MNS (MFEP index 45). Stacking energy is taken to be the energy between the C6 and G7 base pairs. Total energy is the energy of the subsystem comprising IBP, drug, and the largest number of water at any point along the MFEP within 3.4 Å from the heavy atoms of the IBP−drug complex. Each point represents the average value of the members of the biggest cluster around points along the MFEP. (c) Number of hydrogen bonding interactions between the amine groups of proflavine and the IBP. (d) Change in the Buckle of the base pairs C6-G19 and G7-C18 along the MFEP. (e) Number of water molecules around the drug and IBP along the MFEP within 3.4 Å from the heavy atoms. (f) Different base pair parameters of DNA and the direction of the arrow show the sequence of change in the parameters. Standard deviations are shown.

dx.doi.org/10.1021/jp307911r | J. Phys. Chem. B 2012, 116, 12208−12212

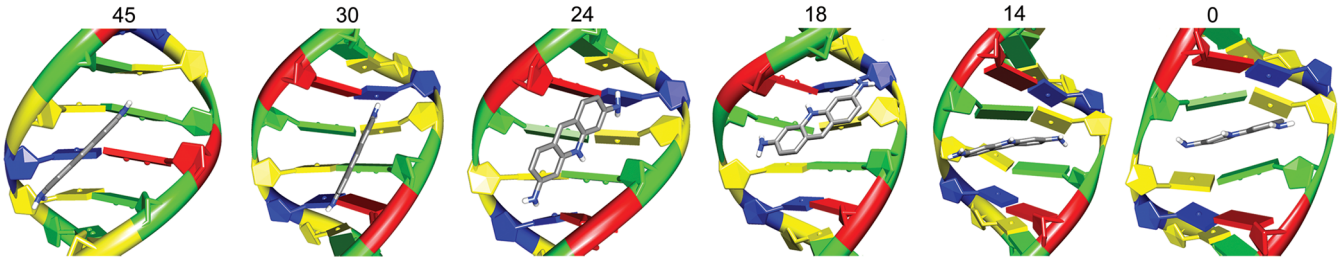

Figure 4. Representative structures along the MFEP (45→0) of the intercalation process. Structures are drawn in chimera.[53] MFEP indices are mentioned on top.

IBP C6G7. The variation in step parameters reflects a sequential process that follows a minimum base-stacking penalty pathway correlated with the position of the drug. Twist is the first DNA parameter to change attaining the lowest value at 31. Here the drug forms a maximum hydrogen bond with the DNA base pairs (Figure 3c) stabilizing Coulombic energy (Figure S2b). Change in Twist is followed by increase in Slide and Shift reaching the maximum at 15. This happens through hydrogen bonding of two amine groups with the sugar oxygen (see structure 18 of Figure 4). Twist in general and Shift and Slide to a certain extent do not cause base-stacking penalty.[46] This is also seen from the unchanged stacking energy (combined vdW and Coulombic energy of the IBP) up to 18 in Figure 3b. The largest shift is followed by a sudden increase of Roll at 14 (thus releasing the linear force into an angular motion), where the drug rotates and inserts like a flap between the base pairs (see video S1). Here base stacking energy increases, however, compensated by the interaction with the drug (Figure 3b). In the final phase of intercalation, Roll and Slide decrease followed by Buckle changing from positive to negative cup (see Figure 3a,d). The presence of proteins and drugs in the intercalation cavity is also known to cause buckling in the DNA.[47] Buckle in a negative cup reflects a sudden increase in Rise. However, Buckle does not cost base-stacking[48] and therefore serves here as a remedial measure to avoid energetically costly Rise. At the final stage, Rise increases resulting in the increase of stacking energy. At this stage, drug−DNA interaction energy decreases stabilizing the total interaction energy. A major energy contribution to the free energy barrier comes from the desolvation energy (Figure 3b) due to the presence of fewer water molecules in the first hydration shell of the IBP (Figure 3e). Rest of the contribution to the free energy barrier may be attributed to entropy.

In summary, this study uses configurational restraint to successfully capture a direct intercalation event in molecular detail for the first time. Analysis of DNA parameters and various energy components along the MFEP indicates that the intercalation of proflavine adopts a minimal base-stacking penalty pathway (Twist→Shift/Slide→Buckle/Roll→Rise) induced by the drug proflavine. Therefore, these results suggest that the mechanism of intercalation for proflavine defies the natural fluctuation hypothesis[49] and supports a drug-induced cavity formation mechanism.[6] It is interesting to note that the importance of Roll angle opening for the deintercalation pathway was shown before by us using a different drug, daunomycin,[15] although the reason for Roll angle opening was not clear. Moreover, correspondence between DNA structural changes and various energy parameters reinforces the minimum base-stacking penalty pathway-mediated intercalation process. Therefore, a similar mechanism (the exact order of parameter variation may differ depending on the structural features of the drug) may be applicable for a general intercalation process. We find here that water plays a major role in controlling the energy component of the intercalation barrier, while the entropy component is most likely dependent on the drug. This requires further investigation using configurational entropy as employed in drug−DNA binding[50] and the intercalation process.[51] Moreover, a complete mechanistic pathway for intercalation and deintercalation through major and minor groove pathways will provide a deeper understanding of the intercalation process.

■ ASSOCIATED CONTENT

Ⓢ Supporting Information

Figures showing time dependence of collective variables, interaction energy graphs, estimate of error and additional FES of intercalation, details of methods, initial coordinates, and video showing mechanism of intercalation. This material is available free of charge via the Internet at http://pubs.acs.org.

■ AUTHOR INFORMATION

Corresponding Author

*E-mail: arnab.mukherjee@iiserpune.ac.in; Phone No.: +91 2590 8051; Fax No.: +91 2589 9790.

Author Contributions

The manuscript was written through contributions of all authors. All authors have given approval to the final version of the manuscript.

Notes

The authors declare no competing financial interest.

■ ACKNOWLEDGMENTS

The authors acknowledge the Indian Institute of Science Education and Research, Pune, for providing the computational facility and funding. The authors thank L. S. Shashidhara for comments on the manuscript.

■ ABBREVIATIONS

IS, intercalated state; MNS, minor groove-bound state; IBP, intercalating base pair; MFEP, minimum free energy path

■ REFERENCES

(1) Lerman, L. S. *J. Mol. Biol.* **1961**, *3*, 18−30.
(2) Berman, H. M.; Young, P. R. *Annu. Rev. Biophys. Bioeng.* **1981**, *10*, 87−114.
(3) Hurley, L. H. *Nat. Rev. Cancer* **2002**, *2*, 188−200.
(4) Brana, M. F.; Cacho, M.; Gradillas, A.; De Pascual-Teresa, B.; Ramos, A. *Curr. Pharm. Des.* **2001**, *7*, 1745−1780.
(5) Werner, M. H.; Gronenborn, A. M.; Clore, G. M. *Science* **1996**, *271*, 778−84.

(6) Li, H. J.; Crothers, D. M. *J. Mol. Biol.* **1969**, *39*, 461−477.
(7) Ramstein, J.; Ehrenberg, M.; Rigler, R. *Biochemistry* **1980**, *19*, 3938−3948.
(8) Bereznyak, E.; Gladkovskaya, N.; Khrebtova, A.; Dukhopelnikov, E.; Zinchenko, A. *Biophysics* **2009**, *54*, 574−580.
(9) Tang, P.; Juang, C. L.; Harbison, G. S. *Science* **1990**, *249*, 70−2.
(10) Neidle, S.; Jones, T. A. *Nature* **1975**, *253*, 284−285.
(11) Nuss, M. E.; Marsh, F. J.; Kollman, P. A. *J. Am. Chem. Soc.* **1979**, *101*, 825−833.
(12) Neidle, S.; Pearl, L. H.; Herzyk, P.; Berman, H. M. *Nucleic Acids Res.* **1988**, *16*, 8999−9016.
(13) Swaminathan, S.; Beveridge, D. L.; Berman, H. M. *J. Phys. Chem.* **1990**, *94*, 4660−4665.
(14) Paik, D. H.; Perkins, T. T. *Angew. Chem., Int. Ed.* **2012**, *51*, 1811−1815.
(15) Mukherjee, A.; Lavery, R.; Bagchi, B.; Hynes, J. T. *J. Am. Chem. Soc.* **2008**, *130*, 9747−9755.
(16) Wilhelm, M.; Mukherjee, A.; Bouvier, B.; Zakrzewska, K.; Hynes, J. T.; Lavery, R. *J. Am. Chem. Soc.* **2012**, *134*, 8588−8596.
(17) Denny, W. A. *Curr. Med. Chem.* **2002**, *9*, 1655−1665.
(18) DeJong, E. S.; Chang, C.-e.; Gilson, M. K.; Marino, J. P. *Biochemistry* **2003**, *42*, 8035−8046.
(19) Barducci, A.; Bussi, G.; Parrinello, M. *Phys. Rev. Lett.* **2008**, *100*, 020603.
(20) Alessandro, L.; Francesco, L. G. *Rep. Prog. Phys.* **2008**, *71*, 126601.
(21) Macke, T.; Case., D. A. *Modeling Unusual Nucleic Acid Structures*; Leontes, N.B., Santa-Lucia, J., Jr., Eds.; American Chemical Society: Washington, DC, 1998.
(22) Wang, J.; Cieplak, P.; Kollman, P. A. *J. Comput. Chem.* **2000**, *21*, 1049−1074.
(23) Perez, A.; Marchan, I.; Svozil, D.; Sponer, J.; Cheatham, T. E., III; Laughton, C. A.; Orozco, M. *Biophys. J.* **2007**, *92*, 3817−3829.
(24) Besler, B. H.; Merz, K. M.; Kollman, P. A. *J. Comput. Chem.* **1990**, *11*, 431−439.
(25) Frisch, M. J.; Trucks, G. W.; Schlegel, H. B.; Scuseria, G. E.; Robb, M. A.; Cheeseman, J. R.; Montgomery, J. A.; Vreven, T.; Kudin, K. N.; Burant, J. C., et al.; *Gaussian 03*, revision C.02; Gaussian, Inc.: Wallingford, CT, 2003.
(26) Case, D. A.; Cheatham, T. E., III; Darden, T.; Gohlke, H.; Luo, R.; Merz, K. M., Jr.; Onufriev, A.; Simmerling, C.; Wang, B.; Woods, R. J. *J. Comput. Chem.* **2005**, *26*, 1668−88.
(27) Cornell, W. D.; Cieplak, P.; Bayly, C. I.; Kollmann, P. A. *J. Am. Chem. Soc.* **1993**, *115*, 9620−9631.
(28) Wang, J.; Wolf, R. M.; Caldwell, J. W.; Kollman, P. A.; Case, D. A. *J. Comput. Chem.* **2004**, *25*, 1157−1174.
(29) Sorin, E. J.; Pande, V. S. *Biophys. J.* **2005**, *88*, 2472−93.
(30) Morris, G. M.; Goodsell, D. S.; Halliday, R. S.; Huey, R.; Hart, W. E.; Belew, R. K.; Olson, A. J. *J. Comput. Chem.* **1998**, *19*, 1639−1662.
(31) Morris, G. M.; Huey, R.; Lindstrom, W.; Sanner, M. F.; Belew, R. K.; Goodsell, D. S.; Olson, A. J. *J. Comput. Chem.* **2009**, *30*, 2785−2791.
(32) Jorgensen, W. L.; Chandrasekhar, J.; Madura, J. D.; Impey, R. W.; Klein, M. L. *J. Chem. Phys.* **1983**, *79*, 926−935.
(33) Press, W. H.; Teukolsky, S. A.; Vetterling, W. T.; Flannery, B. P. Numerical Recipes in FORTRAN; The Art of Scientific Computing, 3rd edition; Cambridge University Press: New York, 1993.
(34) Berendsen, H. J. C.; Postma, J. P. M.; Gunsteren, W. F. v.; DiNola, A.; Haak, J. R. *J. Chem. Phys.* **1984**, *81*, 3684−3690.
(35) Nose, S. *Mol. Phys.* **1984**, *52*, 255−268.
(36) Hoover, W. G. *Phys. Rev. A* **1985**, *31*, 1695−1697.
(37) Parrinello, M.; Rahman, A. *J. Appl. Phys.* **1981**, *52*, 7182−7190.
(38) Tom Darden, D. Y.; Pedersen, L. *J. Chem. Phys.* **1993**, *98*, 10089−10092.
(39) Hess, B.; Kutzner, C.; van der Spoel, D.; Lindahl, E. *J. Chem. Theor. Comput.* **2008**, *4*, 435−447.
(40) Bonomi, M.; Branduardi, D.; Bussi, G.; Camilloni, C.; Provasi, D.; Raiteri, P.; Donadio, D.; Marinelli, F.; Pietrucci, F.; Broglia, R. *Comput. Phys. Commun.* **2009**, *180*, 1961−1972.
(41) Ensing, B.; Laio, A.; Parrinello, M.; Klein, M. L. *J. Phys. Chem. B* **2005**, *109*, 6676−6687.
(42) Ramstein, J.; Leng, M. *Biophys. Chem.* **1975**, *3*, 234−240.
(43) Ciatto, C; D. A., M.; Natile, G; Secco, F; Venturini, M *Biophys. J.* **1999**, *77*, 2717−2724.
(44) Vargiu, A. V.; Ruggerone, P.; Magistrato, A.; Carloni, P. *Nucleic Acids Res.* **2008**, *36*, 5910−21.
(45) Daura, X.; Gademann, K.; Jaun, B.; Seebach, D.; van Gunsteren, W. F.; Mark, A. E. *Angew. Chem., Int. Ed.* **1999**, *38*, 236−240.
(46) Hunter, C. A.; Lu, X.-J. *J. Mol. Biol.* **1997**, *265*, 603−619.
(47) Victor, J.-M.; Ben-Haïm, E.; Lesne, A. *Phys. Rev. E* **2002**, *66*, 060901.
(48) Christopher, A, H. *J. Mol. Biol.* **1993**, *230*, 1025−1054.
(49) Macgregor, R. B.; Clegg, R. M.; Jovin, T. M. *Biochemistry* **1987**, *26*, 4008−4016.
(50) Harris, S. A.; Gavathiotis, E.; Searle, M. S.; Orozco, M.; Laughton, C. A. *J. Am. Chem. Soc.* **2001**, *123*, 12658−12663.
(51) Mukherjee, A. *J. Phys. Chem. Lett.* **2011**, *2*, 3021−3026.
(52) Lavery, R.; Moakher, M.; Maddocks, J. H.; Petkeviciute, D.; Zakrzewska, K. *Nucleic Acids Res.* **2009**, *37*, 5917−5929.
(53) Pettersen, E. F.; Goddard, T. D.; Huang, C. C.; Couch, G. S.; Greenblatt, D. M.; Meng, E. C.; Ferrin, T. E. *J. Comput. Chem.* **2004**, *25*, 1605−1612.